

7-24-2019

Origin and development of true karst valleys in response to late Holocene sea-level change, the Transverse Glades of southeast Florida, USA

John (Jack) Meeder

Peter Harlem

Follow this and additional works at: https://digitalcommons.fiu.edu/serc_fac



Part of the [Life Sciences Commons](#)

This work is brought to you for free and open access by the Southeast Environmental Research Center at FIU Digital Commons. It has been accepted for inclusion in SERC Faculty Publications by an authorized administrator of FIU Digital Commons. For more information, please contact dcc@fiu.edu.



Origin and development of true karst valleys in response to late Holocene sea-level change, the Transverse Glades of southeast Florida, USA

John F. Meeder¹ | Peter W. Harlem^{1,2†}

¹Southeast Environmental Research Center, Florida International University, Miami, Florida

²GIS-RS Center, Florida International University, Miami, Florida

Correspondence

John F. Meeder, Southeast Environmental Research Center, Florida International University, Miami, FL.
Email: jackmeeder@gmail.com

Abstract

The Miami Limestone is an oolite depositional body that is used as an analog model for geological interpretation of the rock record. Barrier-bar complex, oolite banks, extensive bryozoan flats and tidal creeks, referred to as transverse glades, have been described. High-resolution LiDAR data are used to produce unprecedented, detailed topographic maps of the transverse glades in the southern Atlantic Coastal Ridge. These maps were originally used to calculate historic discharge from the Everglades but revealed features inconsistent with the prevailing theory that the topography is of a depositional origin. Field observations verified an epikarst terrain truncated by collapsed subsurface conduits creating valleys, previously described as palaeotidal creeks. Observations of the 12 southern tidal creeks or transverse glades provided a sequence of six stages in the development of these karst valleys. After Late Pleistocene deposition of the Miami Limestone, sea-level dropped producing conditions of: (a) epikarst which reduced the surface elevation preferentially, forming the southern Everglades Basin and modifying Biscayne Bay and Florida Bay precursor basins and (b) downward water movement producing vertical solution features. As Holocene sea-level approached the South Florida carbonate platform margin a freshwater lens formed and groundwater movement became horizontal. Two sets of cavernous zones developed during the Middle and Late Holocene. Solution pipes and dolines provide a connection between the surface and groundwater along alignments which delineate subsurface conduits. Stages of valley formation are associated with the collapse of these conduits first forming a series of pocket valleys followed by narrow blind valleys and half blind or through valleys linking the Everglades to the coastal plain. Valleys then expanded in width until: (a) completion of cavernous zone collapse, (b) most boulder fields and valley margins reduced by weathering and (c) the valleys filled with wetland soils.

KEYWORDS

Everglades, Holocene, karst valley, LiDAR, sea-level, transverse glade

[†]Deceased 15 May 2016

1 | INTRODUCTION

The surface topography of southeast Florida is widely accepted as the original depositional topography, which is reasonable based on the Late Pleistocene age (Halley, Shinn, Hudson, & Lidz, 1977; Hoffmeister, Stockman, & Multer, 1967). However, LiDAR data for the Atlantic Coastal Ridge and coastal plain were collected for storm surge analysis by the International Hurricane Center (Whitman, Zhang, Leatherman, & Robertson, 2003). The processed data are utilized to create the most detailed topographic map and associated elevation profiles of eastern Miami-Dade County, Florida (Zhang et al., 2003; Zhang & Whitman, 2005), for analysis of land loss associated with sea-level rise (Harlem & Meeder, 2008) and as a first step in the calculation of historic freshwater discharge from the Everglades to Biscayne Bay (Meeder & Harlem, 2010). The profiles revealed that topography is not as simple as typical tidal creek or river systems because of the steep, near vertical walls, irregular surfaces, boulder fields and the presence of escarpments and terraces. Field observations confirmed a surface characterized as epikarst interrupted by collapsed subsurface caverns forming valleys. This finding led to several years of further, more intense field investigations on the origin of South Florida topography.

1.1 | Previous work

Although karst features of South Florida are described in numerous works (Cooke & Mossum, 1929; Craighead, 1971; Davis, 1943; Duever et al., 1986; Harshberger, 1914; Parker, 1975; Parker & Cooke, 1944; Parker, Ferguson, & Love, 1955; Sanford, 1909; White, 1970), no studies focused on karst have been conducted except for two studies addressing subsurface cavern distribution (Cressler, 1993; Florea & Yuellig, 2007). In contrast to the world renowned north and central Florida karst systems (Fairbridge, 1968), the karst nature of South Florida is not well-known (Cunningham & Florea, 2009). The small scale (<6 m vertical relief), not the diversity of karst features, may be the reason for the lack of interest. The significance of karst in supplying water has been recognized (Parker et al., 1955) and is still the subject of research (Cunningham et al., 2004, 2006; Cunningham, Renken, et al., 2006; Cunningham, Wacker, et al., 2009; Renken et al., 2005, 2008; Sullivan, Price, Schedlbauer, Saha, & Gaiser, 2014). The role of karst in the origin and evolution of the Everglades ecosystem is not addressed in detail although the sedimentary record is fairly well-known (Gleason & Stone, 1994). The development of the Everglades basal marl (calcite mud) resulted from the precipitation of dissolved carbonate from the dissolution of limestone by biophysio-chemical processes (Gleason & Spackman, 1974). The basal marl is an important controlling mechanism in later

Everglades ecosystem development (Gleason & Stone, 1994; Sklar et al., 2019).

1.2 | Geological setting

Only strata of the Late Pleistocene Miami Limestone composed of oolite, skeletal and minor amounts of quartz sand and silt out crop (Cunningham, Renken, et al., 2006; Parker et al., 1955). Three depositional facies are recognized, namely cross-bedded ooids, bioturbated ooids and bryozoan (Hoffmeister et al., 1967). A distinct unconformity between the Late Pleistocene Miami Limestone and the underlying Pleistocene Fort Thompson Formation, an arenaceous skeletal packstone, is described (Hickey et al., 2010; Perkins, 1977). The historic theory of the origin of the South Florida terrain is that of a depositional origin; the transverse glades had their origin as tidal channels in an oolite shoal (Hoffmeister et al., 1967; Shaler, 1890). The active oolite shoal (present Atlantic Coastal Ridge) developed *ca* 15 km west of a contemporaneous coral reef, the Key Largo Limestone, that extends as far north as Soldier Key in central Biscayne Bay. Further offshore is a recent coral reef that also extends as far north as Soldier Key. Halley et al., (1977) proposed that the outer portion of the Atlantic Coastal Ridge is a later barrier-bar complex deposited against the antecedent oolite shoal system. Neal, Grasmueck, McNeil, Viggiano, and Eberli, (2008) documents two depositional units along the barrier-bar complex using ground penetrating radar, the basal mottled oolitic facies and the upper bedded oolitic facies which is subdivided into two depositional units representing oolitic shoal deposits and barrier-bar formation through alongshore progradation.

This paper focuses on karst valleys produced by collapse of cavernous zones between the Everglades Basin and coastal plain along the water table surface. Numerous valleys in karst terrains have been reported but none of them were created by karst processes alone. Valleys of karst origin are generally considered non-existent and the term karst valley is considered misleading (Sweeting, 1973). The question of the existence of valleys of true karst origin is based upon two well-established concepts: (a) karst drainage is characteristically downwards and (b) valley formation is generally of fluvial origin involving the erosion and transport of materials at the surface. Valleys in karst landscapes are generally classified as either: (a) allogenic or through valleys, formed by rivers with origins in impermeable rocks adjacent to limestone; (b) blind valleys; (c) half-blind valleys; (d) pocket valleys; or (e) dry valleys which form under conditions of glaciation, permafrost, structural or tectonic activity (Sweeting, 1973). The other geological settings forming valleys in karst regions are not observed in South Florida.

1.3 | Purpose and objectives

The purpose of this paper was to document the karst origin of transverse glades by presenting a developmental sequence of morphologies found by LiDAR and verified in the field. The karst origin of the transverse glades offers a new paradigm in contrast to tidal origin. The following objectives are addressed: (a) production of Atlantic Coastal Ridge and transverse glade topography maps; (b) production of Atlantic Coastal Ridge transverse and longitudinal profiles of the transverse glades; (c) production of topographic maps of smaller scale, specific sites; (d) develop an origin for the karst valley model based upon repetitive and sequential topographic profiles; and (e) document the relationship between sea level, freshwater table and karst valley development.

2 | METHODS

The study area included northern Monroe, eastern Collier and southern Broward Counties, but was focused on Miami-Dade County south of the Miami River. The best outcrops were found along the transverse glade valley walls and on remnant exposures (Figure 1). Bodies of limestone left behind after erosion were termed remnants. Most of the Atlantic Coastal Ridge was covered by urban development and a great deal of the transverse glade area was in agriculture or lower density housing thus reducing available outcrops to parks and isolated natural areas. More than 67 field sites were investigated, but only 12 sites were used in this report and cover the variation found in the development of karst valleys (Figure 1 and Table 1).

LiDAR data were collected by the International Hurricane Center for the purpose of studying storm surges along the east coast of South Florida (IHRC {International Hurricane Research Center, Florida International University} 2004). LiDAR data were reduced, removing non-ground measurements and released for public use (Whitman et al., 2003; Zhang et al., 2003; Zhang et al., 2005). These data were used to produce topography maps with >30 cm resolution, far superior to previous topography maps, with precision eliminating the need for most surveying. The site-topography maps produced by LIDAR were used with Atlas GIS software to produce elevation profiles of the Atlantic Coastal Ridge, transverse glades and remnants. These profiles were instrumental in characterizing valley morphology and in the comparison of sites. As many as 12 elevation profiles were made across each transverse glade in order to document topographic trends from the Everglades Basin to the coastal plain. Only one set of transverse elevation profiles are presented as representative of all transverse glades. Karst features such as escarpments and terraces, dolines, hanging valleys and valley margin features were identified. The Atlantic Coastal Ridge longitudinal (long axis) profile was made along the topographic high trend. The

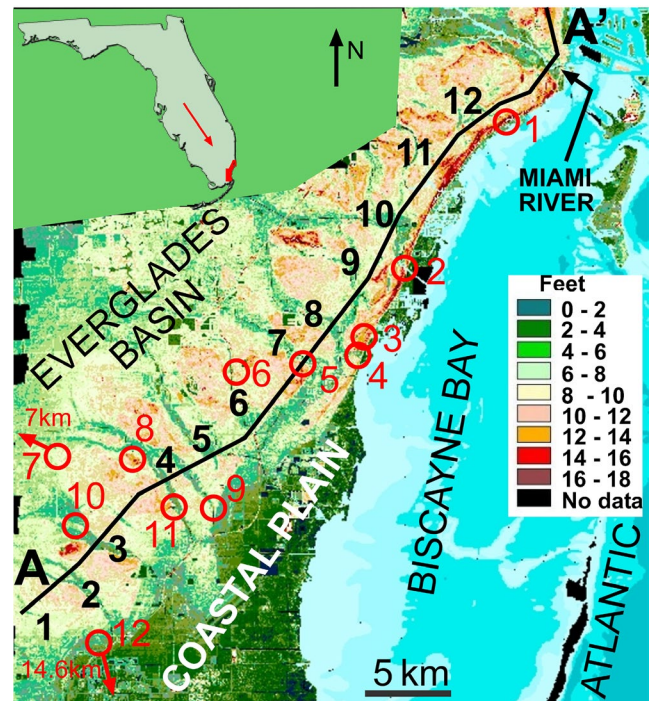


FIGURE 1 LiDAR topography map of southeast Florida with the major geomorphic features labelled. The location of the enlarged LiDAR image is delineated in red with a red arrow in the State image. The transverse glades are numbered in black from south to north, 1-12. Major field sites are numbered corresponding to Table 1. Two red circles with arrows indicate that these sites are located off the map in the direction of the arrow the distance indicated. The location of the longitudinal elevation profile down the axis of the Atlantic Coastal Ridge is indicated by the line A-A'. Water bathymetry is indicated by shades of blue from near shoaling (lightest blue) to ~5 m (dark blue)

longitudinal profiles down the transverse glades established valley bottom topography and slope.

High-quality historic aerial photography (1938), taken prior to most urban development, was utilized allowing observation of many features presently undetectable. Recent aerial photographs were used for easy site location. The source for all aerial photographs was cms.uflib.ufl.edu/maps/collections. Digital cameras were used to document karst features found in the field and for comparison with the LiDAR produced topography. Field measurements consisted of measuring solution feature dimensions for confirmation of LiDAR topography and for correlation of subsurface conduits.

3 | RESULTS

The results from the different methods employed in this study of karst valley genesis are presented by landscape feature and development stage. This method of presentation was selected for ease of use and a better understanding of the development of karst valleys by collating all supporting evidence for each stage, reducing redundancy by presenting all photographs

TABLE 1 Major field and remote study location information

Site	Name	Lat-Long	Street	Ownership
1	Silver Bluff	25.725000° –80.239750°	South of Dinner Key on Biscayne Bay shoreline	Private
2	Snapper Creek	25.665612° –80.279505°	Southeast from Snapper Creek Bridge and Old Cutler Road	Miami-Dade County
3	North of Deering Estate	25.625014° –80.304804°	SW 152 ST	Private
4	Deering Drain	25.622462° –80.303602°	16701 SW 72 Ave	Miami-Dade County
5	Bill Sadowski Park,	25.607897° –80.319579°	17555 SW 79 Ave, Palmetto Bay. By office	Miami-Dade County
6	SW 180 St outcrop	25.60556° –80.319579°	8190 SW 180 St	Miami-Dade County, EEL
7	S of Grossman Hammock	25.564558° –80.575238°	At turn in road	ENP
8	Castellow Hammock	25.558625° –80.452222°	22400 SW 157 Ave	Miami-Dade County
9	Transverse glade 3 sink	25.543643° –80.390667°	12300 SW 240 St	Private
10	Camp Owaissa Bauer	25.523335° –80.468140°	SW 256 St	Miami-Dade County
11	Princeton Prairie	25.542734° –80.409311°	West of Bridge on US 1 just north of SW 248 St	Private
12	Southeast Saline Everglades (along US1)	25.316044° –80.452653°	Along US1 between 10 and 20 km south of Florida City	SFWM

and LiDAR in separate sections then summarizing for each stage. With the exception of historic and aerial photographs, all photographs, LiDAR images produced from source data files and GIS results were original products.

3.1 | Atlantic coastal ridge

A topographic map of the Atlantic Coastal Ridge was made documenting an elevation range from 8.6 m above mean sea level adjacent to the Miami River to little more than 1 m in Everglades National Park (Figure 1). The Atlantic Coastal Ridge was segmented by 12 transverse glades in the study area. The topography between valleys was typical uneven epikarst terrain (Klimchouk, 2004) with abundant doline development (Figure 2). Pillars of outcropping remnant limestone, indicated by very narrow, sharp peaks in the red line between transverse glades, delineated the original depositional surface. Holocene wetland sediments covered both the Everglades Basin and coastal plain on either side of the Atlantic Coastal Ridge (Davis, 1946).

3.2 | Transverse glades

Everglades Basin water delivery to Biscayne and Florida Bays was historically determined by transverse glades.

Transverse glades either crossed or nearly crossed the Atlantic Coastal Ridge and appear as numbered green bands running across the tan Atlantic Coastal Ridge (Figure 1). Transverse glades were irregular in nature and were described in terms of transverse and longitudinal elevation profiles and orientation with respect to the Everglades Basin.

3.2.1 | General characteristics

The Atlantic Coastal Ridge topographic highs and transverse glade floor lows increased in elevation northwards along the profile A–A' (Figure 1). Maximum bank full stage was determined from valley wall elevations and indicated by the upper green line (Figure 2). The historic Everglades stage was determined by the highest elevation of wetland soils along valley flanks (dark blue line, Figure 2). The elevation of the Everglades Basin floor (light blue line, Figure 2) was higher than transverse glade floors (lowest light blue, Figure 2).

3.2.2 | Elevation profiles

Considerable valley morphology variability between and along transverse glades was documented based upon

Atlantic Coastal Ridge and transverse glade topography

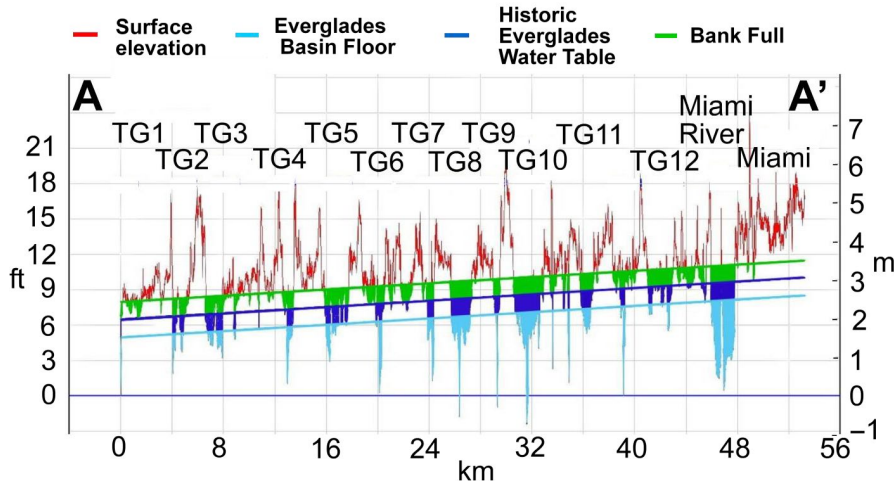


FIGURE 2 An elevation profile (Figure 1, A–A’) down the axis of the Atlantic Coastal Ridge west of the barrier-bar complex (Halley et al., 1977). The red line denotes the elevation of bedrock along the Atlantic Coastal Ridge above the transverse glade bank full stage (green line). The elevation of the transverse glade floor is denoted by the colour filled area, the green area lies between bank full and historic Everglades Basin water table (as defined by distribution of marl), the dark blue defines the area between the historic Everglades water table and the elevation of the Everglades Basin floor and the light blue area denotes the area lying below the floor of the Everglades Basin. These light blue topographic lows were the primary Everglades Basin drains.

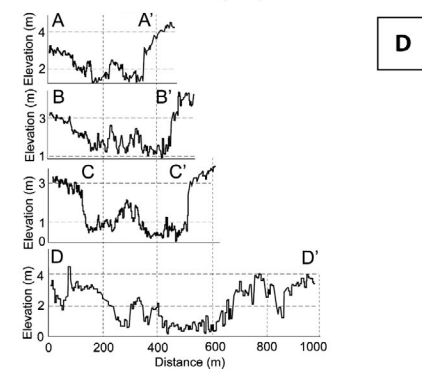
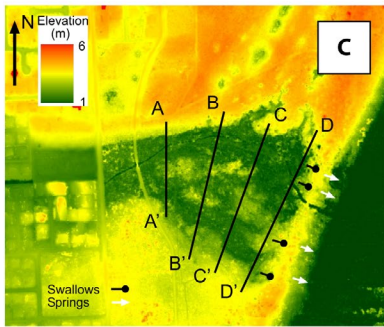
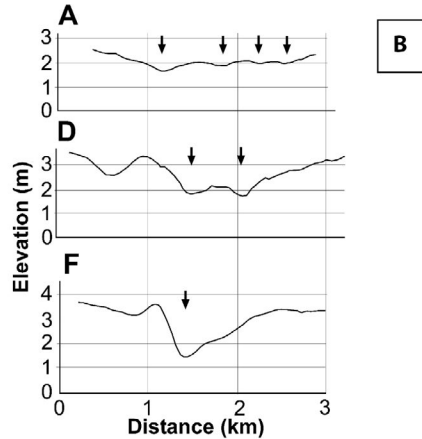
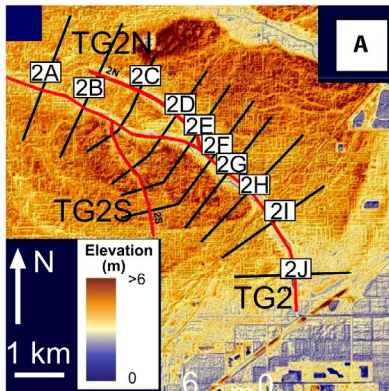


FIGURE 3 (A) LiDAR topography map of Transverse glade 2 (Figure 1) with elevation profile locations. (B) Elevation profiles for Transverse glade 2: profile 2A, 737 m.; profile 2D, 3,230 m; and profile 2F, 3,810 m from Everglades (A). Channels within the transverse glade are indicated by black arrows and decrease in number towards Biscayne Bay. (C) LiDAR topographic map of the Deering Drain (Figure 1, Site 4) with location of elevation profiles, springs (black circles) and swallows (white arrows). (D) Elevation profiles for the Deering Drain from west (A–A’) to east (D–D’).

numerous transverse elevation profiles (Figure 3A). However, three distinct reaches were found in most transverse glades; the western (Everglades Basin margin), central and the eastern (highest portion of the Atlantic Coastal Ridge). The western reaches of transverse glades exhibited broad, shallow profiles, with an irregular epikarst floor frequently

modified by several shallow channels present within the glade (Figure 3B, Profile A, arrows). The limestone surface was reduced by >1 m from the Everglades Basin floor creating the floor of Transverse glade 2. The central reach exhibited two distinct channels and had steeper walls with a terrace (Figure 3B, Profile D, arrows). The Atlantic Coastal Ridge

reach exhibited a single channel with steep walls (Figure 3B, Profile F, arrow). The broad and shallow western valley's transition into steeper and deeper valleys provided evidence of valley wall maturation and further documented valley development towards the east. Some valleys were compound with two steep-walled channels that exhibited lateral expansion by collapse and epikarst deterioration of the limestone ridge separating them, as well as, along the outer valley walls (Figure 3C). These individual channels developed over separate groups of subsurface conduits with the same floor elevations (between 1 and 1.3 m) and were easily observed along the Deering Drain valley floor walls as discontinuous cavernous horizons at the base of escarpments. This process resulted in irregular valley floors covered with boulders and remnants as observed by the very uneven elevation profiles indicative of high relief (Figure 3D).

3.2.3 | Longitudinal elevation profiles

A high degree of variability in transverse glade slope and continuity was documented by the longitudinal elevation profiles (Figure 4). Slopes varied from a continuous slope from the Everglades Basin to the Bay (Transverse glades 3, 4 and 8), sloping to the Everglades from the east (Transverse glades 9 and 11) or were compound, with reversals of slope along the course (Transverse glades 2, 5, 6, 10 and 12). Eight of the 12 transverse glades terminated prior to reaching the coast. These transverse glades were termed half-blind valleys as they have one topographic open end, in contrast to blind valleys which were closed at both ends forming a closed contour (Sweeting, 1973). The elevation of transverse glade floors, at their head at the eastern edge of the Everglades Basin, was 1.8 m in the north and decreased southwards to *ca* 1.2 m. The elevation at the coastal plain ranged between 1.2 and 0.9 m, respectively. Variation in slopes included: continuous slopes from the Everglades Basin to the Bay (Transverse glades 3, 4 and 8), slopes from the Coastal Ridge to the Everglades Basin (Transverse glades 9 and 11), or were compound, with reversals of slope along their courses (Transverse glades 2, 5, 6, 10 and 12).

3.2.4 | Orientation of transverse glades

The transverse glades exhibited a general NW–SE orientation along the Atlantic coastline and trended in more southerly directions in the westernmost Atlantic Coastal Ridge reach (Figure 5). Most transverse glades appeared to radiate outwards from the centre of the southern Everglades Basin.

3.3 | Documentation of karst valley development

A six-stage conceptualization of karst valley development was formulated (Figure 6 and Table 2) and described and

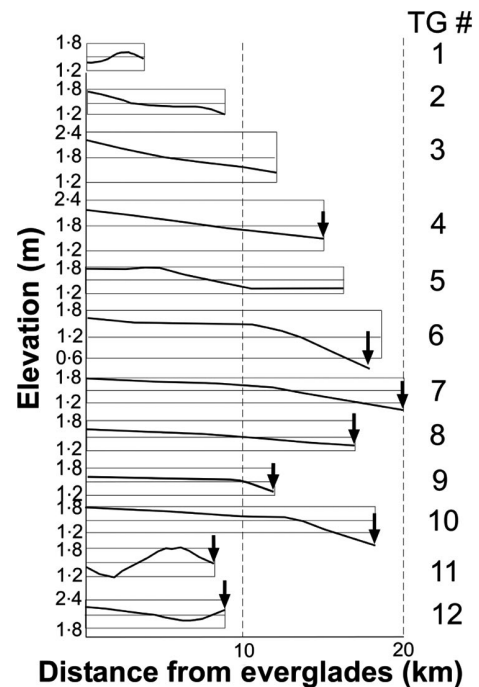


FIGURE 4 Longitudinal elevation profiles were made along the bottom of each transverse glade from the Everglades Basin (left) to the coastal plain (right). Transverse glade (TG) numbers correspond with locations presented in Figure 1 and Table 1. Transverse glades that terminate prior to completely traversing the Atlantic Coastal Ridge form half-blind valleys that usually end at swallows, marked with a downward arrow

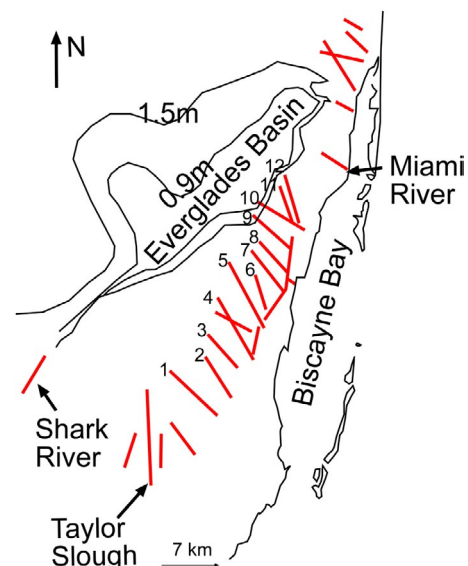


FIGURE 5 Orientation of transverse glades (red lines) and their relationship to the Everglades Basin. (Topography of Everglades Basin modified from Parker et al., 1955.)

discussed in chronological order (Figures 7–12). Each developmental step in each stage has been located on the model (Figure 6) by a corresponding numbered dashed line box. Field, (2002) and Sweeting, (1973) provided karst definitions.

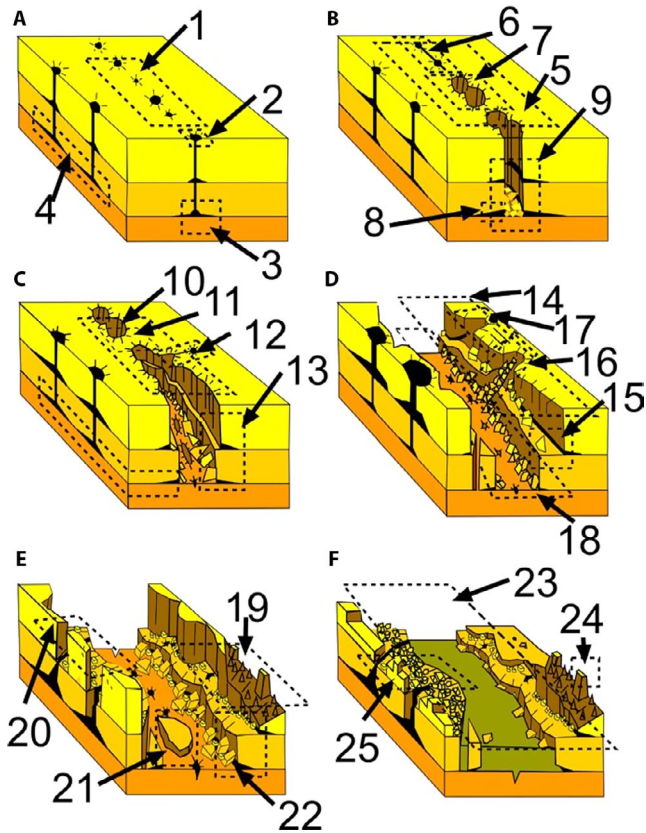


FIGURE 6 Schematic illustration of the six stages of karst valley development. The letters correspond to the stages as described and illustrated in Results. Areas outlined in dashed lines are illustrated in the corresponding figure as numbered. The three strata represent hypothetical limestone units and the dark strata within the valley (F) is Holocene marl sediment. Early sedimentation beginning during Stage B consisted of minor amounts of quartz sand derived from dissolution of the arenaceous oolitic limestone but was replaced by wetland marl sediment

TABLE 2 Summary of Karst Valley development

Stage	Figure	Landscape feature	Other
A	7	Alignment of solution pipes and dolines	
B	8	Series of pocket valleys	First observable conduits
C	9	Narrow blind valleys	First hanging valleys
D	10, 11	Half blind or through valleys	First terraces
E	12	Widening valley	Valley outliers
F	13	Sediment fill	Reduced relief

3.3.1 | Stage A

Alignments of dolines and solution pipes were identified and located over subsurface conduits (Figure 6A). The relationship between the dolines and solution pipes with subsurface conduits was not observable in expansive wetlands because

of sediment burial and overlying scrub cover. However, this relationship was confirmed in uplands such as the Castellow Hammock and Camp Owaissa Bauer (Figure 1, Sites 8 and 10) and exposed in later stages of development after collapse of subsurface conduits. Horizontal conduits developed with a slight dip towards the coast. Such alignments of dolines were found throughout the Big Cypress Swamp (Duever et al., 1986), Southeast Saline Everglades (Ross, Sah, Meeder, Ruiz, & Telesnicki, 2013) and the central and southern Everglades Basin and were usually filled with Holocene sediment and identified by the overlying tree islands (Figure 7A). Dolines were observable as topographic depressions throughout the eastern Everglades Basin and Atlantic Coastal Ridge. Both solution and collapse dolines were very common in linear alignments; some dolines exhibited radiating fractures (Figure 7B). Subsurface cavernous zones were not readily observed in Stage A and ranged from simple ovate shaped conduits like those reaching Biscayne Bay (Figure 7C) to wide, irregular stratiform cavernous horizons, usually with little headroom, best observed at the base of collapse valley walls (Figure 7D). Alignments of collapse dolines were also found on large remnant limestone outliers (Figure 7E). The profile (A–A') down the axis of aligned dolines displayed the epikarst surface and depths and distribution of dolines over the conduit (Figure 7E and F). Doline floor elevations varied little (0.7–1.3 m) with most variation the result of the presence of boulders or minor sediment fill. Foot caves were visible in many instances.

3.3.2 | Stage B

Expansion of dolines and coalescence into elongate, frequently barbell shaped, pocket valleys established Stage B valleys from their precursors (Figures 6B and 8A). Stage B valleys were long, narrow, discontinuous steep-walled valleys with floors covered by large boulders (Figure 8A). The development of fractures between solution pipes and dolines was common (Figure 8B). A profile (Figure 8C) displayed valley floor roughness (Figure 8A, A–A'). Coalescing dolines were easily separated from individual dolines by their greater width and topographic irregularity. An elevation profile displayed the steep collapse walls and the deep epikarst at the surface (Figure 8D). Horizontal cavernous zones were first observed during this stage as foot caves (Figure 8E), in many instances buried under collapse boulders and debris (Figure 8F).

3.3.3 | Stage C

Further collapse resulted in widening and coalescence of pocket valleys forming longer, steep-walled half blind to blind Stage C valleys (Figure 9A). The Snapper Creek site exhibited Stage C valley characteristics broadest at the Biscayne Bay shoreline

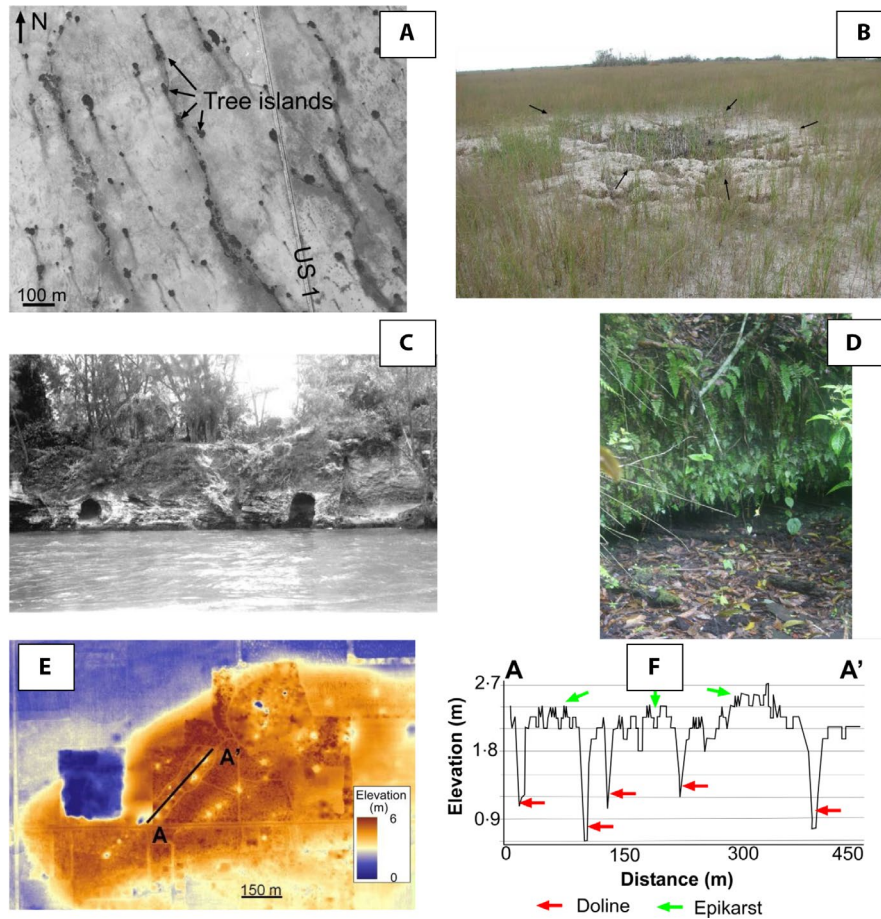


FIGURE 7 Stage A. (A) 1938 aerial photograph of the Southeast Saline Everglades along US 1 (Figure 1, Site 12) showing the distribution of tree islands, the majority overlying bedrock depressions as in many areas (Duever et al., 1986). Bedrock depressions along US 1 vary in depth and larger islands frequently developed in depressions 1.5 m deep with the 2.5 m depressions within 200 m of Biscayne Bay. Most bedrock depressions are in linear or slightly arching alignments and range in depth from 0.6 to 2.5 m (Figure 6A, Inset 1). (B) Photograph (Figure 6A, Inset 2) of a doline *ca* 7 m in diameter partially filled with Holocene marl sediment exhibiting a radial fracture pattern south of Grossman Hammock (Figure 1, Site 7). Radial fractures indicated by arrows. (C) A series of caverns (Figure 6A, Inset 3) exposed along Silver Bluff (Figure 1, Site 1). Photograph copied from W. Armstrong Price (1953). (D) A near continuous cavernous zone 40 cm in height (Figure 6A, Inset 4) exposed as a foot cave along a Stage B valley wall, Castellow Hammock (Figure 1, Site 8). (E) The Bauer Hammock within the Camp Owaissa Bauer (Figure 1, Site 10) is an outlier with elevations between 2 and 5 m above the surrounding transverse glade. Topography of the Bauer Hammock (Figure 6A, Inset 1) exhibits alignments of dolines (Figure 1, Site 10). The blue box in the western region is borrow pit. (F) An elevation profile (Figure 7E, A–A') documents the linear alignment of dolines and a very irregular epikarst surface (Figure 6A, Inset 1)

with a spring head, the origin of Snapper Creek, rapidly reduced width westwards, disappearing at the Atlantic Coastal Ridge into a series of dolines connected to subsurface conduit. Snapper Creek developed in the opposite direction of most valleys. The floor was near sea level. Collapse occurred either evenly in two directions or in one direction more than another (Figure 9A, north-east side of valley shown in the lower south-east part of the figure). Immature valleys terminated at a series of collapse dolines (Figure 9A, north of the coalescing pocket valleys) or at swallows (Figure 9B). A swallow is where surface water enters the subsurface draining a pocket or half-blind valley as a point source, usually a solution hole. Major transverse glades either crossed the Atlantic Coastal Ridge, were terminated at the outer ridge of the Atlantic Coastal Ridge as

swallows (Figures 1 and 4), or changed course to disappear at swallows (Figure 9B). Arches were occasionally still in place where two pocket valleys were incompletely coalesced (Figure 9C). Hanging valleys were developed along older valley walls. Hanging valleys resulted in deterioration of older valley walls and valley expansion by sudden collapse (Figure 9D) or by collapse of a honeycomb of high density, small-scale solution pipes (Figure 9E). The Snapper Creek outlet was a series of large spring heads (Figure 9F).

3.3.4 | Stage D

Dissolution and collapse of rock above the cavernous horizons resulted in development of terraces and escarpments

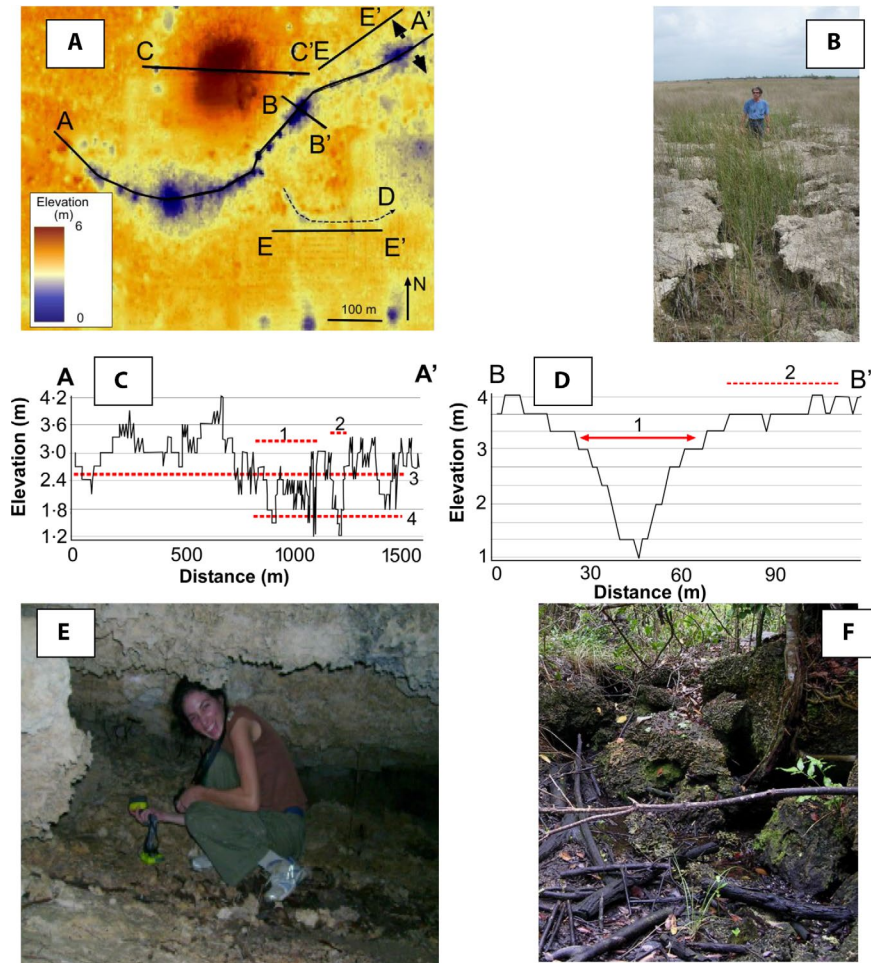
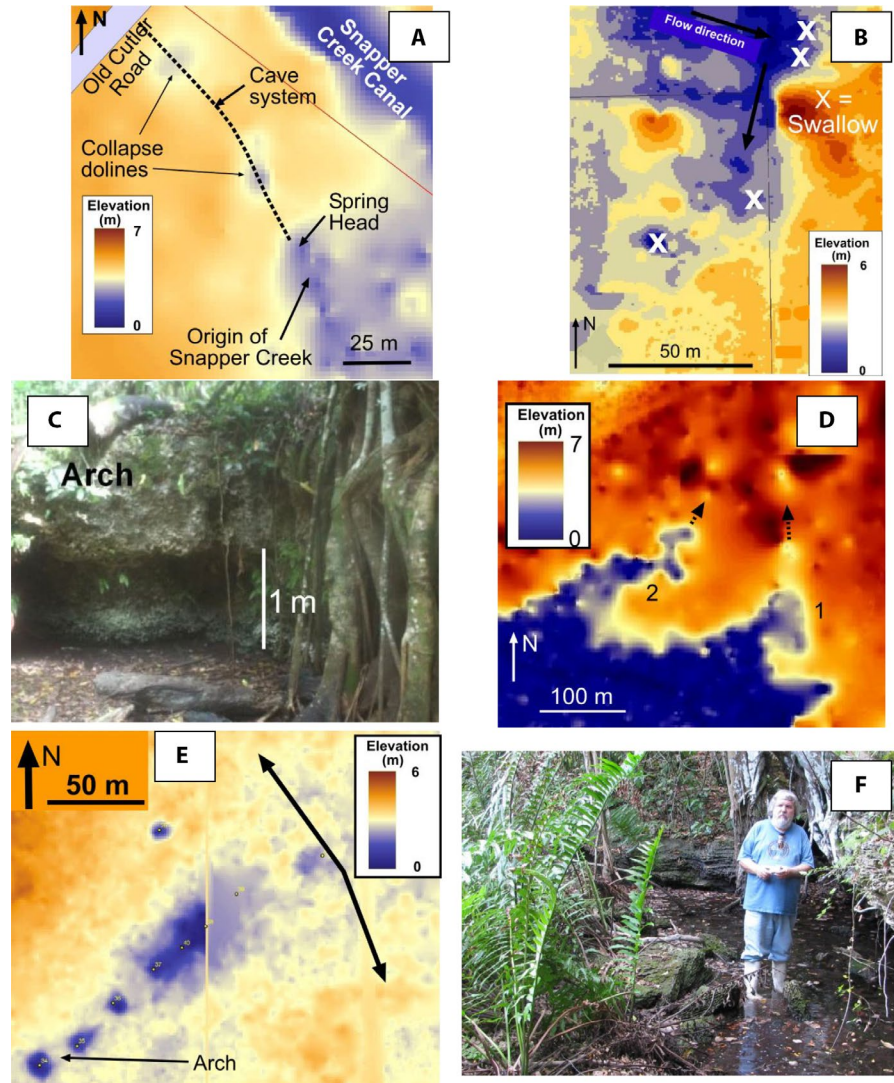


FIGURE 8 Stage B. (A) LiDAR topography map of the western part of Castellow Hammock (Figure 1, Site 8) displays a long sinuous valley (A–A'), a set of coalescing dolines (B–B'), a large remnant 5.1 m in elevation (C–C'), a potential very early developing valley or perhaps the remains of a tidal channel (dashed line labelled D) and an area of laterally expanding valley between the two E–E' lines. The area between the two E–E' lines is mottled yellow–orange pattern recording an unstable honeycombed area that threatens collapse and valley width expansion (Figure 6B, Inset 5). (B) A marl-filled fracture expanded by dissolution south of Grossman Hammock (Figure 1, Site 7) linking solution holes and dolines *ca* 5 m in circumference (Figure 6B, Inset 6). (C) Elevation profile down the axis of the series of dolines (Figure 8A, A–A'). A large set of coalescing dolines (1) and a single large collapse doline (2) are easily distinguished from one another. The upper cavernous zone (3) is associated with the surface of the upper terrace development as the loss of limestone above the cavernous zone expands the terrace and in the same fashion as limestone loss above the lower cavernous zone (4) expands the valley floors (Figure 6B, Inset 7). (D) Elevation profile across a valley (Figure 8A, B–B') is composed of coalescing collapse dolines. The elevation profile displays a doline (1) widening towards the top by wall fracture, slumping and dissolution. A well-developed, deep epikarst is developed (2) on either side of the doline (Figure 6B, Inset 7). (E) The Deering Drain (Figure 1, Site 4) exhibits the lower cavernous zone which is very well-developed in places and crawlable (Figure 6B, Inset 8). (F) A typical early collapse valley at Bauer Hammock (Figure 1, Site 9). Valley wall is near vertical and 2.3 m in height with floor covered by large boulders (Figure 6B, Inset 9)

between cavernous zones and above the upper cavernous horizons along widening valley walls (Figure 10A). Three near horizontal surfaces (the transverse glade floor, lower and upper terraces) were visible. An escarpment between the upper two terraces was slightly more than a metre in relief (Figure 10B). Each terrace had an irregular surface from solution of limestone, solution holes and the presence of remnant boulders. Terraces developed as limestone above a cavernous zone were lost by dissolution and collapse creating a flat area littered with boulders. Hanging valleys along the main valley margins became common in some areas (Figure

10C, Inset A documented two hanging valleys). These hanging valleys were younger than the main valleys and were also formed by collapse (Figure 10D). Hanging valleys in their early development were suspended above the main valley floor but eventually developed to the lower cavernous zone, the floor of the main valley (Figure 10E, A–A'). A collapse doline was displayed at the head of this valley. Many hanging valleys had the appearance of swales, as found in ridge and swale complexes associated with barrier island depositional environments (Figure 10F). These valley floors developed a series of solution holes and dolines, perhaps originating in

FIGURE 9 Stage C. (A) LiDAR topography map of Snapper Creek (Figure 1, Site 2), a typical Stage 3 valley (Figure 6C, Inset 10). (B) LiDAR topography of the terminal or box end of the half-blind karst valley, Transverse glade 5 (Figure 1, Site 9), with swallows marked by x's and surface water diversion eastwards and southwards marked by arrows. (C) An arch between two dolines at Bauer Hammock (Figure 1, Site 8). The cavern is *ca* 90 cm in height (Figure 6C, Inset 11). (D) LiDAR topography map of hanging valleys along the northern Deering Drain wall (Figure 1, Site 4) formed by sudden collapse (Figure 6C, Inset 12). (E) LiDAR topography map of the end of the Stage B valley at Castellow Hammock (Figure 1, Site 8) terminated in a highly 'honeycombed' area prior to the margin of a transverse glade (same position as Figure 6C, Inset 12). (F) Peter Harlem standing on the boulder-covered valley floor (Figure 6C, Inset 13) at the spring head and origin of Snapper Creek (Figure 1, Site 2)



precursor swale topography (Figure 11A). Stage D valley floors (Figure 11B, Profile B–B') were uneven, the roughness less than in Stage C valleys but more than found in later stages. Valley width expanded as the steep walls continued to fracture (Figure 11C) and collapse (Figure 11D). This was the first stage when valleys occasionally traverse the entire Atlantic Coastal Ridge. Most valleys however were blind or half-blind, many ending at swallows prior to reaching the coastal plain (Figure 4). Stage D valleys were frequently compound valleys displaying two parallel channels merging into a single valley with maturation (Figure 3B, Profile D; Figure 3C and D, profiles A–D). Valley walls at this stage were very irregular (Figure 10C). The area between the two valley channels consisted of remnant outcrops, boulder fields and exposed upper cavernous zone.

3.3.5 | Stage E

Valleys that had widened and deepened to near their full potential or reached near total collapse of the

underlying cavernous zones were considered mature, Stage E valleys. Valley walls were much less steep with less relief. Reduced relief was the result of valley floor elevation rising in response to wetland sedimentation and the final stages of wall collapse and continued epikarst development (Figure 12A). Hanging valleys had broadened, in many areas greatly reducing the valley wall height and slope (Figures 9E and 12B). Occasional large remnants were found a metre or more in elevation above the valley floor (Figure 12C). Hardwood hammocks developed on these isolated remnants surrounded by wetland soils. Valley floors are more level with boulders only observed along the valley walls. Some wetland sediment filling had begun as the valleys were wide enough that shading from trees no longer prohibited wetland vegetation growth and marl or peat soil accumulation. Terraces and escarpments were well-developed along valley margins or were almost unrecognizable as they decomposed by dissolution and filled with organic debris (Figure 12D).

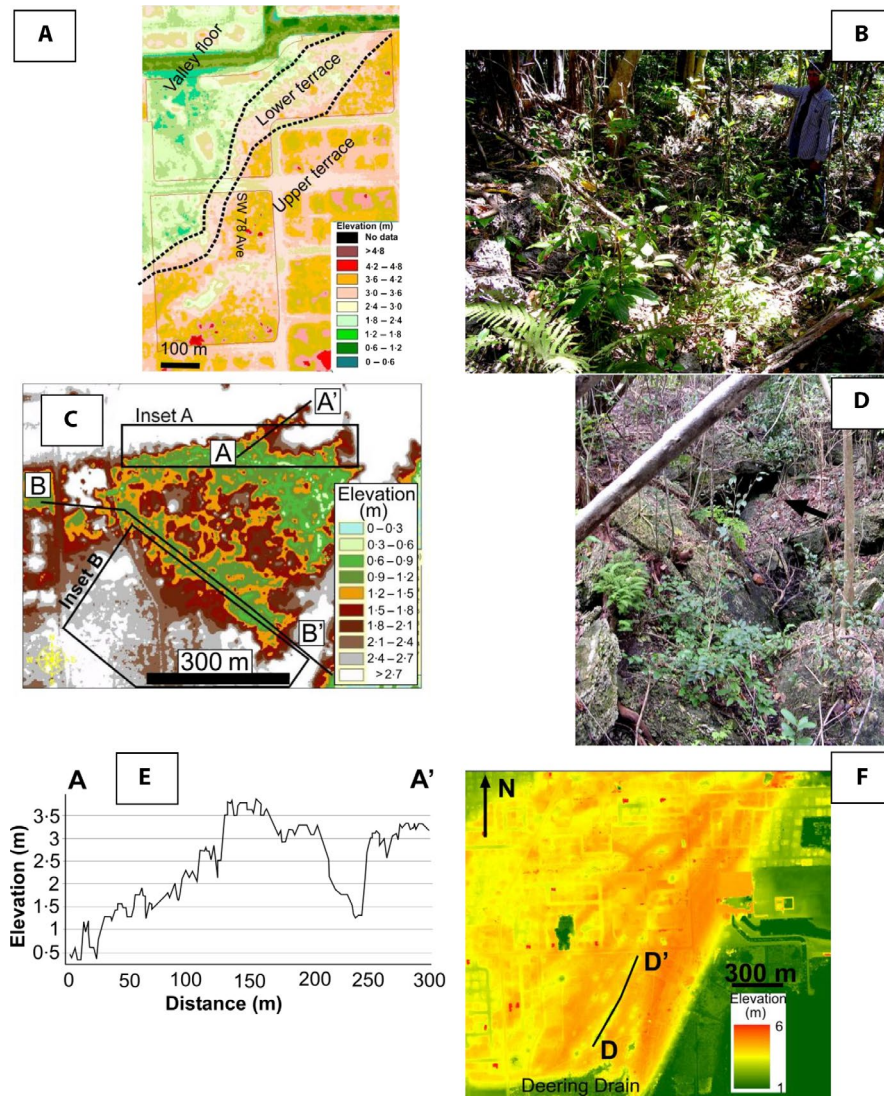


FIGURE 10 Stage D. (A) LiDAR topography map of Sadowski Park (Figure 1, Site 5) along the edge of Transverse glade 7 illustrates well-developed terraces (Figure 6D, Inset 14). (B) Upper terrace along the upper escarpment at Sadowski Park (Figure 6D, Inset 15). (C) LiDAR topography map of the Deering Drain (Figure 1, Site 4) showing a valley with two channels (green) which are both expanding laterally. The scale used here is to emphasize the roughness of the valley walls (Inset A) and the deterioration of the upper terraces (Inset B). The area around transect A–A' is a collapse hanging valley (Figure 6D, Inset 18). (D) Photograph looking up the axis of a hanging valley (Figure 6D, Inset 16) at the Deering Drain. Arrow points to cavern opening *ca* 1 × 3 m in dimensions. (E) Elevation profile along the axis of a hanging valley (Figure 10C, A–A') with a large collapse doline in the alignment (Figure 6D, Inset 17). (F) LiDAR topography map of the area immediately north of the Deering Drain (Figure 1, Site 3) displaying swale like depressions visible as yellow bands (Figure 6D, Inset 16). Transect D–D' runs down the axis of a swale

3.3.6 | Stage F

Continued erosion and valley filling resulted in reduced valley relief in the final stage of valley development. Most transverse glades exhibited some sediment filling along reaches, especially in the west, and others were filled from wall-to-wall with marl (Figure 13A). Surface erosion frequently left behind small scale but high relief pillars (Figure 13B). Epikarst processes reduced the valley margins in both elevation and relief burying the lower caverns with boulders, organic debris, sand and marl (Figure 13C). At this stage rapid, continued valley development became a localized activity. Cessation of active

karst processes and sediment filling began at the margin of the Everglades Basin and developed eastwards because valley formation first began at the edge of the Everglades Basin and moved eastwards with groundwater. The slope of the valley wall generally decreased with increased age of the valley.

4 | DISCUSSION

4.1 | Atlantic coastal ridge

The Atlantic Coastal Ridge is of depositional origin (Halley et al., 1977) the question is how much of the present topography

FIGURE 11 Stage D continued. (A) Elevation profile (Figure 10F, D–D') down the axis of a 'swale' (Figure 6, Inset 16). (B) Elevation profile (Figure 10C, B–B') down the axis of the southern valley floor at Deering Drain (Figure 1, Site 4) retaining characteristics of a blind valley (Figure 6D, Inset 18). (C) A large fracture 4 m in length (Figure 6, Inset 17), continuing out of sight, running parallel to the south valley wall at the Deering Drain (Figure 1, Site 4). (D) Remnant limestone outcrop between valley channels *ca* 1.5 m in height (Figure 6D, Inset 15) at the Deering Drain (Figure 10C, between green contour intervals)

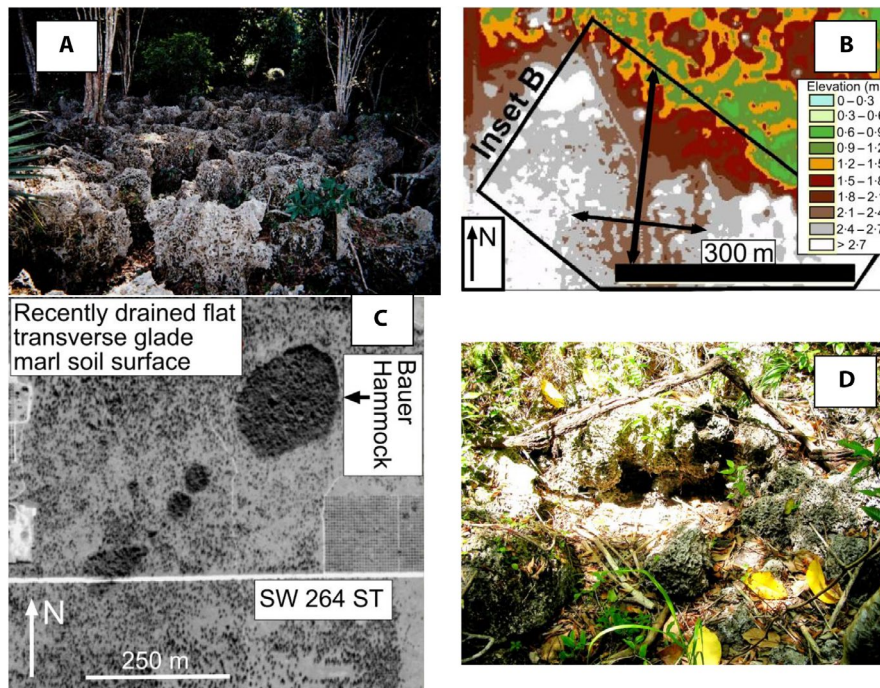
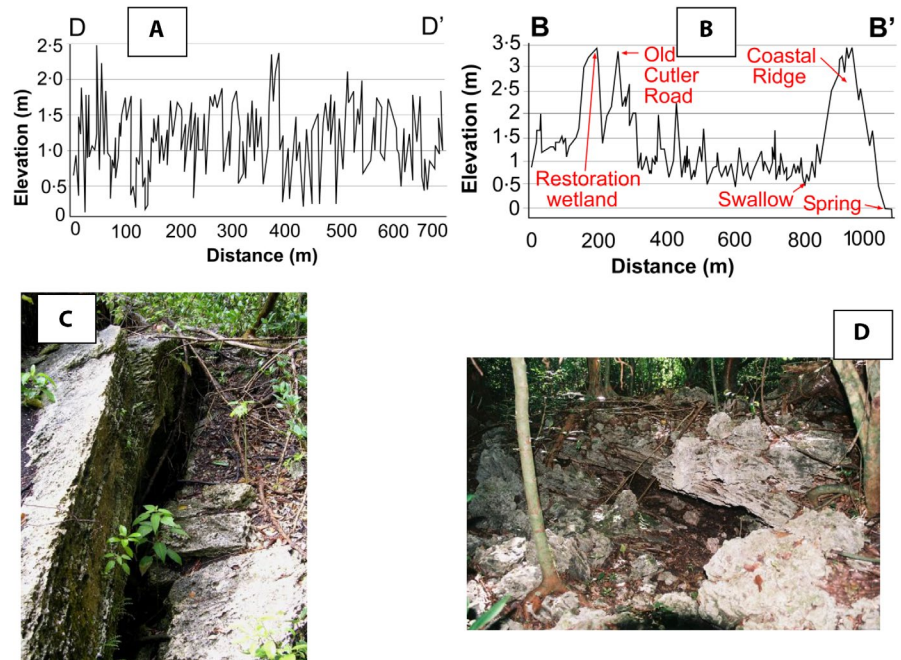


FIGURE 12 Stage E. (A) Photograph of well-developed epikarst with 0.75 m relief (Figure 6E, Inset 19) along valley margin (Figure 1, Site 6). (B) LiDAR topography map of a highly decomposed (mottled white and grey contour intervals) hanging valley (Figure 10C, Inset B) along the south wall of Deering Drain (Figure 1, Site 4). Arrows indicate direction of valley expansion or valley wall decomposition (Figure 6E, Inset 20). (C) 1938 aerial photograph of Camp Owaissa Bauer, Bauer Hammock is the large remnant on the transverse glade floor covered by hardwood hammock (Figure 6, Inset 21). The elevation of the Hammock is up to 5 m above the surrounding valley floor which is partially filled with wetland marl soils. (D) Highly decomposed valley wall at Sadowski Park (Figure 1, Site 5) with distinct cavernous zone exposed *ca* 40 cm in height, covered with boulders and filled with sediment and organic detritus (Figure 6E, Inset 22)

is the result of deposition and how much from erosion processes? The surface of the Atlantic Coastal Ridge is an epikarst surface characterized by remnants and pillars dispersed

throughout the study area documenting between 1 and 3.3 m (Figure 1, Sites 4, 5 and 8) of surface limestone lost along the Atlantic Coastal Ridge axis (Figure 13B). Large remnants of

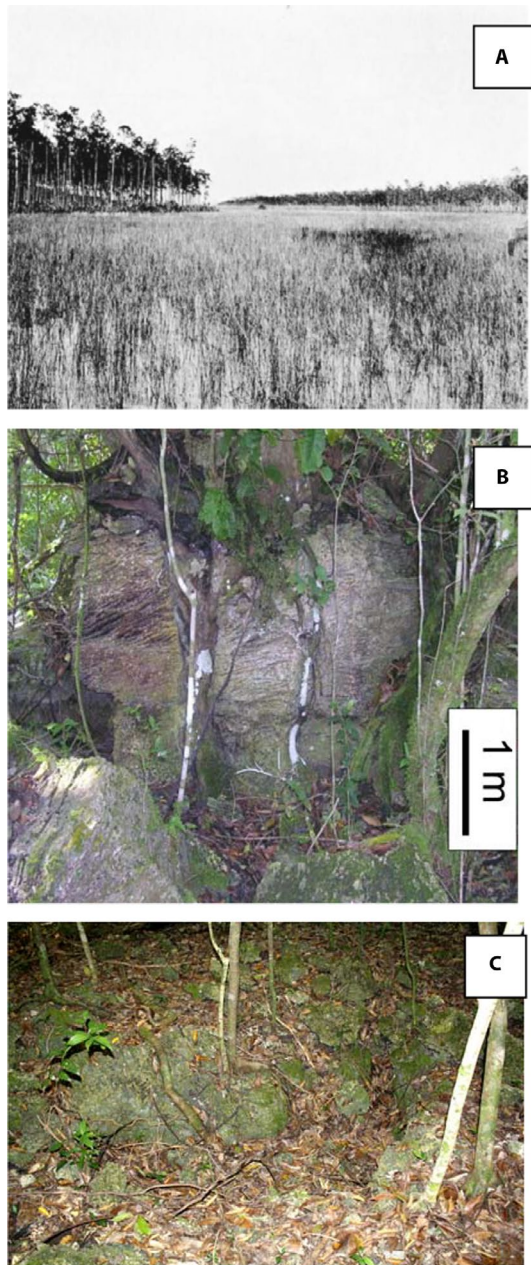


FIGURE 13 Stage F. (A) Aerial photograph (*ca* 1900 Miami-Dade Historic Society) of Princeton Glade, Transverse glade 3 (Figure 1, Site 10). Valley filled with *ca* 1 m of Late Holocene marl sediment. The valley margin is very gradational into the upland pine forest (Figure 6F, Inset 23). (B) Photograph of bedrock remnant forming pillar (Figure 6F, Inset 24) along valley margin at the Deering Drain (Figure 1, Site 4). (C) Photograph of highly decomposed valley wall at Sadowski (Figure 1, Site 5). Note small size of boulders compared to earlier valley stages (Figure 10D). The relief along the valley wall is <35 cm, marl sediment is in the foreground and organic litter is beginning to accumulate. Lateral valley expansion by collapse ceased as the terminus of the cavernous system was reached (Figure 6F, Inset 25)

up to 5.1 m in elevation are found 24 km west of the present day ridge (Figure 1, Site 8), along the eastern margin of the Everglades Basin (Figure 8A, line A). The Everglades Basin

development was by limestone dissolution at the expense of much of the original Atlantic Coastal Ridge (active shoal) limestone body. Limestone loss was at the surface, one layer after another, as well as in the subsurface. Limestone remnants in many cases exhibit the loss of four to five distinct depositional strata in a step-like manner, perhaps analogous to escarpments and terraces at a larger scale along valley walls (Figure 10B) documenting the lowering of the basin by 1.5 m or more (Figure 1, Site 7). The base of many remnants in the Everglades Basin approached the average depth of the Everglades Basin. The present Atlantic Coastal Ridge also extended further east under Biscayne Bay to a distance of at least 1,000 m from the western shoreline (Byrne, 1999). The presence of this oolitic limestone has not received attention. Cross-bedded strata overlie mottled strata along the Atlantic Coastal Ridge (Neal et al., 2008). Because cross-bedded sediments grade westwards into mottled sediments, the presence of the lower mottled strata suggest the presence of cross-bedded strata to the east based upon Walther's Rule. However, the only oolitic sediments present east of the present Atlantic Coastal Ridge is the thin strata found under Biscayne Bay suggesting considerable transport and erosion. Hoffmeister et al., (1967) first postulated oolitic limestone loss from in front of the Atlantic Coastal Ridge. Cross-bedded oolitic limestone remnants up to 1.5 m in height above the background elevation of 2.5 m are found in the eastern Big Cypress National Preserve and further document the loss of considerable limestone (Duever et al., 1986). Therefore, the present narrow Atlantic Coastal Ridge is the remnant of a precursor, broader, active oolite shoal both to the east and west and the entire Everglades Basin has broadened and deepened through karst processes.

The Atlantic Coastal Ridge is made up of two ridges sub-parallel to the coastline, best defined north of Site 6 (Figure 11). The outer ridge is interpreted as a barrier-bar system (Halley et al., 1977). In some areas along the Atlantic Coastal Ridge, ridge and swale deposition occurred (Figure 1, Site 3) which focused karst processes to the swales resulting in development of a series of dolines forming early stage karst valleys. These valleys, with near vertical walls and floors littered with collapse boulders, highly alter the depositional topography. These early stage karst valleys intersect larger karst valleys forming hanging valleys which expand by collapse resulting in the expansion of valley length and width.

4.2 | Transverse glade

The abundance of data suggests that the transverse glades are karst in origin or have been so modified by karst processes as to have removed all morphologic evidence of tidal origin. Original tidal channels have been removed by surface erosion of up to 3 m of the upper Miami limestone. Everglades Basin documenting a minimum loss between 2 and 3 m based

upon remnant outcrops within the Everglades and in the eastern Big Cypress Swamp (Dutton, Carlson, Long, Milne, & Raymo, 2015).

4.2.1 | Large scale observations

The Atlantic Coastal Ridge is dissected by large karst valleys, transverse glades, that are in most cases half-blind valleys (Figure 1). Nearly 35% of the Atlantic Coastal Ridge length is actually occupied by low-lying transverse glade topography (Figure 2). The association between foot caves and associated collapse features with the transverse glade valley walls suggests that the transverse glades are of karst origin.

4.2.2 | Transverse elevation profiles

Transverse glades generally have the flattest, widest profiles in their western reaches adjacent to the Everglades Basin (Figure 1). The transverse glades deepen and narrow towards the axis of the Atlantic Coastal Ridge. Usually along a central reach, two channels can be found in the transverse glade valley. Valley wall slopes are highly variable but, in general, are steepest in the reaches through the highest areas of the Atlantic Coastal Ridge. Valley walls are frequently step-like because of the presence of terraces. Tidal creeks do not form terraces and escarpments. The changing elevation profiles suggest that the karst valleys originated to the west and developed towards the east. The lower relief profile indicates a more mature and more reduced surface (Figure 4B). Over time, the valley profiles become less rough as valley walls are reduced and boulders on the floor decompose. Valleys begin to fill with wetland marl soil, first to the west moving eastwards with valley widening. The elevation of marl soils in the transverse glades are used to determine pre-drainage water table and coincides with the elevation of the upper cavernous horizon (Figure 2, upper surface of dark blue areas delineated by the dark blue line). Bank full flow is indicated by the upper surface of the green areas delineated by the green line (Figure 2). Bank full conditions are rare since the advent of artificial drainage and implementation of active water management. The authors witnessed 1.5 m of water running over Tennessee Road where it crosses Princeton Glade with current velocities of 35 cm sec^{-1} during the ‘Storm of the Century’, March 1994. The light blue line indicates the elevation of the Everglades Basin floor and light blue areas delineate the area of transverse glades below the Everglades Basin floor and corresponds to the elevation of the lower cavernous horizon.

4.2.3 | Longitudinal topographic profiles

The variability in longitudinal profiles is a response to karst valley maturity and is not the result of tidal action process over a shoal (Figure 5). Termination of valleys at sinks

occurs in eight of the 12 transverse glades studied. Arches or evidence of past arches are found at several localities as well as along Arch Creek, to the north. The floors of the transverse glades generally are at 1–2 m above msl, decreasing southwards at the margin of the Everglades Basin and about 0.9–1.2 m at the coastal plain. This coincides with the elevation of the lower cavernous zone. Ten out of 12 transverse glades slope towards Biscayne Bay the tidal source, in contrast to modern ooid shoals that slope towards the platform interior, (Harris & Purkis, 2019; Hoffmeister et al., 1967). Additionally, no transverse glade exhibits tidal deltaic deposits at their terminus.

4.2.4 | Orientation

Transverse glades form a radiating pattern from the axis of the Everglades Basin (Figure 5) following the original groundwater movement from the Everglades Basin towards base level and forming along groundwater flow lines as conduits collapsed. A few small scale linear depressions run from NE to SW and form hanging valleys along a few transverse glades and may be the remains of tidal creeks (Figure 8A, dashed line D). Most of these possible tidal channels are unavailable for observation because of urbanization.

4.2.5 | Scale

Tidal creeks in most ooid shoals are less than a few metres in depth with respect to the top of the active shoal. Since limestone loss of up to 3 m can be documented in large areas and up to 5 m locally, it is assumed that evidence for most of the active tidal channels is now missing. In addition, the elevation of the top of the active shoal is usually within a few metres of that of the adjacent inactive shoals, whereas the difference in elevation in the Miami Limestone is as great as 6 m. The widths of tidal creeks in modern oolite shoals vary with the setting, but usually do not make up 35% of the surface area of a shoal as transverse glades do along the Atlantic Coastal Ridge (Harris & Purkis, 2019). In contrast to transverse glades, tidal channels in modern oolite shoals slope towards the interior basin and produce sub-tidal sediment deltas (Hoffmeister et al., 1967).

4.3 | Karst valley origin and development

Six developmental stages of the karst valleys are presented (Figure 6). Most individual karst valleys exhibit two or three stages of development along their reaches; however, the sequences of development are repetitive between transverse glades. The development of karst valleys is demonstrably tied to prior development of shallow subsurface cavernous conduits connecting the Everglades Basin to the coastal

basins. Sea level, geology and freshwater supply determines the position of the freshwater lens which control cavern development.

4.3.1 | Origin of cavernous horizons

The karst development of southeast Florida topography is tied to freshwater availability and sea level which controls the carbonate platform groundwater table (Figures 14 and 15). Freshwater is the agent of dissolution and in limestone regions rapidly infiltrates bedrock moving downward to the water table. Two sides of the Biscayne Aquifer are exposed along the platform margins to ocean conditions. The Biscayne Aquifer is an eogenetic karst environment (Cunningham, Renken, et al., 2006; Vacher & Mylroie, 2002) which is represented by the 'simple island' model (Jenson et al., 2006). Carbonate island karst develops in young, relatively unaltered limestone units with high-primary porosity. The Miami limestone has relatively high primary porosity (*ca* 25%) which has increased through dissolution and diagenesis to >40% exhibiting an extremely high transmissivity (Fish & Stewart, 1991). Carbonate island karst is further defined by the effects of differential dissolution associated with the contacts between vadose-freshwater phreatic groundwater and fresh-marine water mixing zone. Caverns are best developed along the vadose-phreatic contact where fresh rain water is under saturated in terms of Ca (Plummer, 1975). Solution conduits are used to indicate palaeo sea-level positions (Mylroie & Carew, 1988). The migration of the mixing zones in response to glacio-eustatic and tectonic variations in relative sea level is recorded by the elevation of cavernous zones developed during corresponding sea levels. The freshwater lens is elevated by the denser sea water, therefore the upper surfaces of cavernous horizons are slightly elevated above the groundwater sea-level stand during which they developed and have a slight seaward dip in areas with a significant freshwater lens. The timing of cavern development is based upon: (a) rapid Late Pleistocene sea-level regression; (b) sea level never reaching elevations high enough to affect platform near surface water table during the Early Holocene; (c) very minimal debris or sediment filling; and (d) a lack of 'dripstones' or other cave formation development suggesting immature Middle and Late Holocene caves. The timing of cavern development is linked to the periods of time when the groundwater surface was above present sea level.

4.3.2 | Geological history

The six stages of karst valley development are related to changes in geological environments from the original

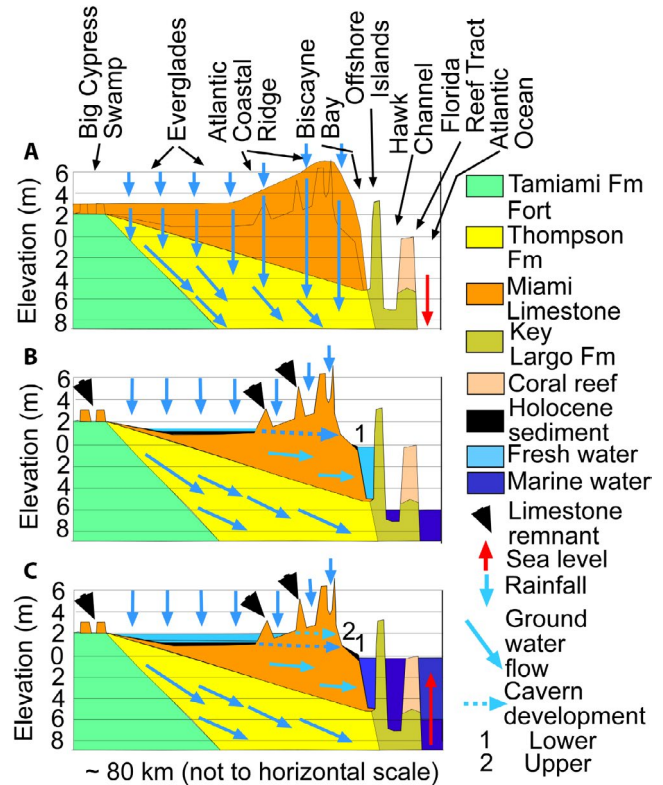


FIGURE 14 Key hydrologic conditions for the development of South Florida topography and karst valleys. (A) Post-depositional low sea-level stand (11,700 yr BP) and the Late Pleistocene (120,000 yr BP) depositional surface. The Miami Limestone (orange) is divided by a line representing the present land surface and the postulated overlying post-depositional surface. Rainfall (light blue lines above illustrations) infiltrates the porous bedrock and travels vertically as groundwater (subsurface light blue arrows). Groundwater moves along bedding planes and exposure horizons prior to reaching the low water table associated with the last glacial low sea-level stand. (B) Middle Holocene (6,000 yr BP) sea-level rise and inundation of the Everglades Basin. Sea level at the beginning of the Middle Holocene was within 6 m of present sea level which was sufficient to raise platform groundwater to the point of Everglades Basin inundation (light blue) and wetland marl deposition (black). Present day sea level is represented by 0 in the elevation scale bars. Prior epikarst processes resulted in the development of the Everglades and Biscayne Bay basins and reduction of surface along the Atlantic Coastal Ridge as suggested by limestone remnants (Note the limestone loss in A). Groundwater movement became near horizontal (light blue arrows) as the freshwater lens developed over rising denser sea water. Horizontal groundwater movement along the vadose-freshwater phreatic boundary resulted in intensified dissolution and cavern development from the base of the Everglades Basin thru the Atlantic Coastal Ridge to the coastal plain (light blue dashed arrow labelled 1). (C) Continued sea-level rise and resultant historic high freshwater stage. As sea-level rose to near present levels, the freshwater stage rose to its historic high of 3 m above present sea level (light blue) in the Everglades Basin. A second cavernous zone (light blue dashed arrow labelled 2) developed along the new higher vadose-freshwater phreatic boundary)

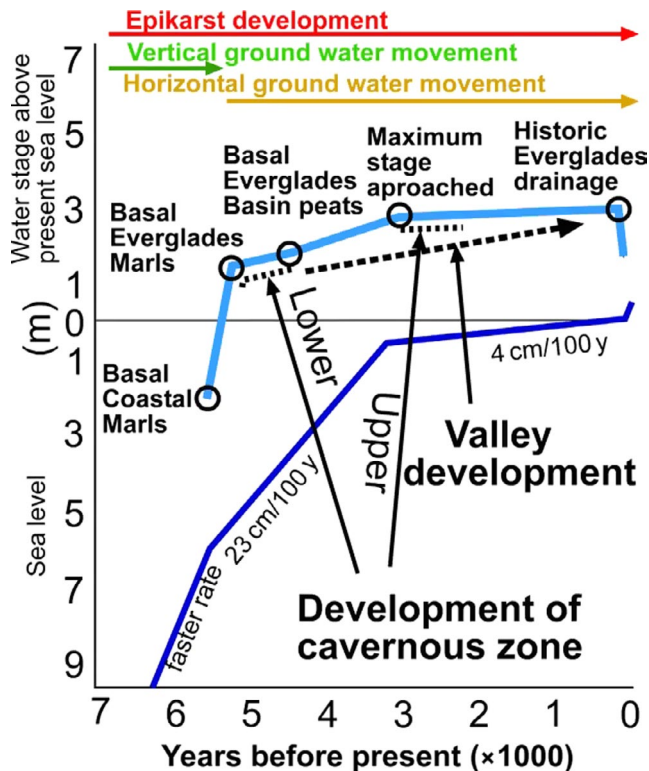


FIGURE 15 Relationship between sea level, platform margin, freshwater table and cavern development. The dark blue line is the late Holocene sea-level curve (modified from Wanless et al., 1994). The freshwater stage or table of the platform is in light blue. This curve is developed from radiometric dates of coastal and Everglades Basin wetland soils (Gleason & Stone, 1994). The timing of five major events is indicated by circles. Periods of epikarst development (red arrow), vertical (green arrow) and horizontal (orange arrow) groundwater movement are indicated along the top. The major periods of cavern development are indicated by dashed lines. The period of karst valley development is indicated by the dashed arrow. The sea-level and groundwater table curves nearly parallel one another after 6,000 yr BP with *ca* 4 m of separation 6,000 yr BP and *ca* 3 m 1,000 yr BP

depositional setting followed by a major post-depositional drop in sea level exposing the carbonate platform. The Holocene transgression began 11,700 yr BP raising the platform water table until the maximum stage was reached. Karst valleys developed during the latter 6,000 yr BP prior to drainage which began in *ca* 1880 (McVoy, Said, Obeysekera, Van Arman, & Dreschel, 2011) lowering the water table and exposing many karst features.

Sea level was at *ca* 8 m above present during the last interglacial *ca* 120,000 yr BP inundating the entire platform during deposition of the Miami Limestone strata (Moore, 1982) although this elevation does not consider the lost elevation of the Atlantic Coastal Ridge. There must have been a strong cross-bank current analogous to the 'Quick Sands' area (Shinn, Lidz, & Holmes, 1990) and the mid Pliocene (Klaus, Meeder, McNeill, Woodhead, & Swart, 2017). Currents

were, at least episodically, sufficient to produce cross-bedded ooid sets 30–80 cm thick west of the Atlantic Coastal Ridge and to transport ooids into Collier County (Figure 1, Sites 6, 8). The ooid shoal developed behind a fringing coral reef, the Key Largo Limestone (Hoffmeister & Multer, 1968). The ooid limestone body begins in northern Broward County and extends *ca* 34 km west of Florida City, the quartz sand content rapidly decreases southwards.

Sea-level dropped rapidly to >120 m below present after deposition, not to rise higher than 6 m below present until approximately 6000 yr BP (Wanless, Parkinson, & Tedesco, 1994). The dominant post-deposition processes were epikarst and vertical dissolution processes with minor development along bedding planes (Figures 14A and 15). During this time interval, the Everglades Basin and Biscayne Basin formed by epikarst processes and the Atlantic Coastal Ridge was reduced in width and height (all limestone above the dark line within the Miami Limestone is lost, Figure 14A). There was little standing water although rainfall may have been abundant because of rapid downward percolation.

Sea level was at least 120 m below present during glaciation and epikarst dominated the Florida Platform between deposition and *ca* 6,000 yr BP when the rate of sea-level rise slowed and when sea-level approached the platform margin (Robbin, 1984). This period of surface erosion lowered the limestone surface everywhere and produced the Everglades and Biscayne Bay basins (Figures 14B and 15). Rising sea-level elevated the freshwater lens inundating the Everglades Basin providing a marl depositional environment (Gleason & Stone, 1994). The marl soils deposited are a product of precipitation of calcium carbonate from dissolved limestone (Gleason & Spackman, 1974). The marls form a leaky seal on the Everglades floor (Figure 14B) slowing water infiltration and storing water, increasing the hydroperiod and providing an environment suitable for peat deposition which started *ca* 4,500 yr BP (Gleason & Stone, 1994) at elevations between 1 and 1.3 m above present sea level (Wanless et al., 1994). Groundwater flow patterns became horizontal, moving south and eastwards resulting in the development of complex conduits, or horizontal cavernous zones, along the vadose-freshwater phreatic contact forming a slight seaward dip along the upper surface of the freshwater lens. This surface and the subsequent cavernous zone ran from the base of the Everglades Basin to *ca* 1 m above sea level along the seaward margin of the Atlantic Coastal Ridge, a drop of *ca* 1 m with respective elevation increases northwards.

Early observations document the Everglades' stage was at 3 m inland from Coconut Grove (Shaler, 1890). The historic high-water stage occurred prior to drainage when the water stage was between 0.6 and 2 m higher than present in the study area (McVoy et al., 2011; Parker, 1975; Parker et al., 1955). This high stage was the product of abundant rainfall

and sea-level rising to within 1 m of present mean sea level 3,000 yr BP at which time the rate of sea-level rise declined to $<1 \text{ mm yr}^{-1}$ (Figures 14C and 15). During this short interval of 3,000 yr, the upper cavernous zone developed (Figure 14C, dashed light blue arrow labelled 2) by the same process as the earlier, lower cavernous system (Figure 14B, dashed light blue arrow labelled 1), at both a higher sea level and freshwater table. The maximum Everglades stage first occurred *ca* 1,200 yr BP (Brooks, 1974) and existed until drainage defining the period of most intense upper cavernous horizon development. The upper cavernous zone is not as well-developed as the lower cavernous zone, probably because the lower cavernous zone was still active during upper cavernous zone development, pirating under saturated water.

Karst valleys formed by collapse of shallow subsurface groundwater conduits. These conduits developed along the vadose-freshwater phreatic boundary forming cavernous horizons. These conduits presumably developed along groundwater paths of least resistance from the Everglades Basin to the coast. Solution pipes and dolines are found in lineaments overlying the subsurface conduits. It is difficult to pinpoint the timing of collapse and valley development, but it is soon after conduit development. Prior to karst valley development, the southern Everglades stage was controlled by southward surface flow and eastward groundwater flow through the Atlantic Coastal Ridge. Groundwater flow supported scores of springs along the Atlantic Coastal Ridge, coastal plain and under Biscayne Bay. After karst valley development, the Everglades stage was controlled dominantly by surface water discharge through the karst valleys and secondly, by groundwater. Water flow via the subsurface conduits occurred until drainage in the 20th Century. Based upon weathering of clasts (decreased size and angularity) and the presence of large mature trees (Figure 9C), the period of active collapse has passed. The following three patterns of cave collapse are recognized: (a) the uppermost strata collapse into the upper cavernous zone forming a terrace; (b) the entire rock section collapsing into the lower cavernous zone forming vertical collapse walls; and (c) the intermediate rock strata collapse into the lower cavernous zone with the upper strata forming the ceiling to a cavern or arch. The floors of most solution pipes are at the same elevation as the floor of the lower cavernous zone.

Drainage of the Everglades has exposed both sets of cavernous zones, now separated by between 1 and 2 m of rock. Exposure of caverns has created air pockets potentially rejuvenating collapse over existing cavernous horizons.

4.3.3 | Review of karst valley development stages

The documentation and description of the six stages of karst valley development are presented (Figures 7–13) and used

to produce a model (Figure 6). Karst valley development is summarized in Table 2. Karst valleys developed as subsurface caverns formed along palaeowater tables collapsed, collapse usually beginning at the Everglades Basin margin then progressing eastwards. The majority of karst valleys never reached Biscayne Bay but disappeared into swallows. These valleys originated entirely by karst processes.

5 | CONCLUSIONS

The Atlantic Coastal Ridge is highly modified by epikarst and subsurface collapse karst processes. Up to a few metres of upper strata has been removed and much of the western Atlantic Coastal Ridge reduced to form the Everglades Basin. Valleys that cut across the Atlantic Coastal Ridge were formed by the collapse of conduits between the Everglades and coastal basins. Epikarst and collapse of shallow subsurface karst have altered the depositional landscape and freshwater delivery from the Everglades to the coastal basins. Valley formation takes place in six described stages, from the origin of subsurface conduits to their collapse and later sediment filling (Figure 6). The best evidence of karst valley origin is the collapse nature of valley walls, exposure of subsurface conduits, the presence of arches indicative of incomplete collapse, the presence of terraces, sinks located at the blind end of many valleys, orientation and profiles inconsistent with tidal creek morphology. No evidence for the tidal origin of the transverse glades was found with palaeotidal channels possibly removed along with the upper 2–3 m of limestone by dissolution.

These karst valleys have formed within the past 6,000 yr in response to rising sea level and a corresponding rise in the freshwater table. Cavernous horizons with a slight dip seaward formed along the vadose-freshwater phreatic contact at two different intervals of sea level. These cavernous zones, a complex network of conduits, radiated outwards from the Everglades Basin axis towards base level. Their collapse and evolution into valleys changed the water delivery patterns to the near shore environment and controlled the Everglades stage.

ACKNOWLEDGEMENTS

We would like to thank Steve Roberts for his extensive help in the field; Dr. Randall Parkinson, Samuel Reese and Peter Stone for reviewing versions of the manuscript and shared numerous conversations; James Brown aided with illustrations; and Drs. Robert N. Ginsburg, Jennifer Richards and Mike Ross shared valuable discussions and aided in the field. We also thank personnel of the Environmentally Endangered Lands and the Miami-Dade Parks and Recreation Departments for access to study sites, especially Molly Messer and Jennifer Tisthammer, respectively. We would like to thank the

reviewers for making this a better manuscript and extend the thanks to the Southeastern Environmental Research center, Florida International University for office and computer support. This research is privately funded. This is contribution number 913 from the Southeast Environmental Research Center in the Institute of Water & Environment at Florida International University.

DATA AVAILABILITY STATEMENT

The data that support the findings of this study are available from the corresponding author upon reasonable request.

REFERENCES

- Brooks, H. K. (1974). Lake Okeechobee. In P. J. Gleason (Ed.), *Environments of South Florida: Present and past*. Miami, FL: Miami Geological Society, Memoir 2, pp. 256–286.
- Byrne, M. J. (1999). Groundwater nutrient loading in Biscayne Bay, Biscayne National Park, Florida. FIU Electronic Theses and Dissertations, 2029. Retrieved from <http://digitalcommons.fiu.edu/etd/2029>.
- Cooke, C. W., & Mossom, S. (1929). Geology of Florida. Florida Geological Survey, 20th Annual Report: 29–227. Retrieved from <http://ufdc.ufl.edu/UF00000051/00001>
- Craighead, F. C. (1971). *The Trees of South Florida, Vol. 1. The natural environments and their succession*. Coral Gables, FL: University of Miami Press. 212 pp. 10:087024146X. ISBN 13: 9780870241468.
- Cressler, A. (1993). The caves of Dade County, Florida. Georgia underground: Dogwood City Grotto Inc, National Speleological Society, 30, 9–16.
- Cunningham, K. J., Carlson, J. L., Wingard, G. L., Robinson, E., & Wacker, M. A. (2004). Characterization of aquifer heterogeneity using cyclostratigraphy and geophysical methods in the upper part of the karstic Biscayne Aquifer, southeastern Florida. United States Geological Survey, Water Resources Investigation Report, 03–4208, 1–66. Retrieved from https://sofia.usgs.gov/projects/index.php?project_url=aq_heterogeneity
- Cunningham, K. J., & Florea, L. J. (2009). The Biscayne aquifer of Southeastern Florida. Caves and karst of the USA. Retrieved from http://works.bepress.com/lee_florea/5/
- Cunningham, K. J., Renken, R. A., Wacker, M. A., Zygnerski, M. R., Robinson, E., Shapiro, A. M. ... Wingard, G. L. (2006). Application of carbonate cyclostratigraphy and borehole geophysics to delineate porosity and preferential flow in karst limestone of the Biscayne Aquifer, SW Florida. *Geological Society of America Special Papers*, 404, 191–208. [https://doi.org/10.1130/2006.2404\(16\)](https://doi.org/10.1130/2006.2404(16)).
- Cunningham, K. J., Sukop, M. C., Huang, H., Alvarez, P. F., Curran, H. A., Renken, R. A. ... Dixon, J. F. (2009). Prominence of ichnologically influenced macroporosity in the karst Biscayne Aquifer: Stratiform “super-K” zones. *Geological Society America Bulletin*, 121, 164–180. <https://doi.org/10.1130/B26392.1>.
- Cunningham, K. J., Wacker, M. A., Robinson, E., Dixon, J. F., & Wingard, G. L. (2006). A cyclostratigraphic and borehole geophysical approach to development of a three dimensional conceptual hydrogeologic model of the karstic Biscayne aquifer, southeastern Florida. U.S. Geological Survey. Scientific Investigations Report, 2005–5235, 1–69. <https://doi.org/10.3133/sir20055235>.
- Davis, J. H. Jr (1943). The natural features of Southern Florida, especially the vegetation, and the everglades. *Florida Geological Survey, Geological Bulletin*, 25, 1–311. Retrieved from http://cescos.fau.edu/gawliklab/papers/Davis%201943-intro_a.pdf
- Davis, J. H. Jr (1946). The peat deposits of Florida, their occurrence, development and uses. *Florida Geological Survey, Geological Bulletin*, 30, 1–247.
- Duever, M. J., Carlson, J. E., Meeder, J. F., Duever, L. C., Gunderson, L. H., Riopelle, L. A. ... Spangler, D. P. (1986). The big cypress national preserve. National Audubon Society Research report no.8, 1–455.
- Dutton, A., Carlson, A. E., Long, A. J., Milne, G. A., & Raymo, M. E. (2015). Sea-level rise due to polar ice-sheet mass loss during past warm periods. *Science*, 349(6244), 4019–4019. <https://doi.org/10.1126/science.aaa4019>.
- Fairbridge, R. W. (1968). *Encyclopaedia of Geomorphology*. New York, NY: Reinhold, 1295 pp.
- Field, M. S. (2002). A lexicon of cave and karst terminology with special reference to environmental karst hydrology. US Environmental Protection Agency, EPA/600/R-02/003, 214 pp.
- Fish, J. E., & Stewart, M. (1991). Hydrogeology of the surficial aquifer system, Dade County, Florida. United States Geological Survey. Water-Resources Investigations Report, 90–4108, 1–50. <https://doi.org/10.3133/wri904108>.
- Florea, L., & Yuellig, A. (2007). Everglades National Park – Surveying the southeastern most cave in the continental United States. *Inside Earth*, 10(1), 3–5. Retrieved from https://digitalcommons.wku.edu/geog_fac_pub/6
- Gleason, P. J., & Spackman, W. (1974). Calcareous periphyton and water chemistry in the Everglades. In P. J. Gleason (Ed.), *Environments of South Florida: Past and present*. Miami, FL: Miami Geological Society, Memoir 2, pp. 225–248. ASIN: B001L0008S.
- Gleason, P. J., & Stone, P. (1994). Age, origin, and landscape evolution of the Everglades peat land. In S. M. Davis, & J. C. Ogden (Eds.), *Everglades: The ecosystem and its restoration*. Delray Beach, FL: St Lucie Press, pp. 149–197. ISBN: 0-9634030-2-8-8.
- Halley, R. B., Shinn, E. A., Hudson, J. H., & Lidz, B. H. (1977). Pleistocene barrier bar eastward of Ooid Shoal Complex near Miami, Florida. *American Association Petroleum Geologists*, 61, 519–526. Retrieved from <http://archives.datapages.com/data/bulletins/197779/data/pg/0061/0004/0500/0519.htm>
- Harlem, P. W., & Meeder, J. F. (2008). Lidar Detection of karst landforms in Miami-Dade County, Florida: a tool for environmental management (Poster). Greater Everglades Ecosystem Restoration (GEER) Conference, Naples, FL. Retrieved from <http://conference.ifas.ufl.edu/GEER2008>.
- Harris, P., & Purkis, S., (2019) New geological perspectives of the Pleistocene Miami Oolite. Fieldtrip Guidebook, Robert Ginsburg Legacy Symposium. Comparative Sedimentology Laboratory, University of Miami, Coral Gables, FL 46p.
- Harshberger, J. W. (1914). The vegetation of south Florida, south of 27° 30' north, exclusive of the Florida Keys. *Wagner Free Institution Science Philadelphia, Transactions*, 7, 51–189.
- Hickey, T.D., Hine, A.C., Shinn, E.A., Kruse, S.E. and Poore, R.Z. (2010) Pleistocene Carbonate Stratigraphy of South Florida: Evidence for High-Frequency Sea-Level Cyclicity. *Journal of Coastal Research*, 26, 605–614. <https://doi.org/10.2112/JCOASTRES-D-09-00052.1>.

- Hoffmeister, J. E. K., & Multer, H. G. (1968). Geology and origin of the Florida Keys. *Geological Society America Bulletin*, 79, 1487–1502. [https://doi.org/10.1130/0016-7606\(1968\)79\[1487:GAOOTF\]2.0.CO;2](https://doi.org/10.1130/0016-7606(1968)79[1487:GAOOTF]2.0.CO;2).
- Hoffmeister, J. E. K., Stockman, W., & Multer, H. G. (1967). Miami limestone of Florida and its recent Bahamian counterpart. *Geological Society America Bulletin*, 78, 175–190. [https://doi.org/10.1130/0016-7606\(1967\)78\[175:MLOFAI\]2.0.CO;2](https://doi.org/10.1130/0016-7606(1967)78[175:MLOFAI]2.0.CO;2).
- IHRC (International Hurricane Research Center, Florida International University). (2004). Windstorm Simulation & Modeling Project. Airborne LIDAR Data and Digital Elevation Models in Broward County, Florida. Final Report. Prepared for: The Broward County Emergency Management Division, 201 N. W. 84 Avenue Plantation, Florida 33324. Retrieved from http://www.ihrc.fiu.edu/wp-content/uploads/2012/05/Broward_FinalReport.pdf
- Jenson, J. W., Keel, T. M., Mylroie, J. R., Mylroie, J. E., Stafford, K. W., Taboroši, D. ... Wexel, C. (2006). Karst of the Mariana Islands: the interaction of tectonics, glacio-eustasy, and freshwater/seawater mixing in island carbonates. *Geological Society America Special Papers*, 404, 129–138. [1130/2006.2404\(11\)](https://doi.org/10.1130/2006.2404(11)).
- Klaus, J. S., Meeder, J. F., McNeill, D. F., Woodhead, J. F., & Swart, P. K. (2017). Expanded Florida reef development during the mid-Pliocene warm period. *Global and Planetary Change*, 152, 27–37.
- Klimchouk, A. (2004). Towards defining, delimiting and classifying epikarst: Its origin, processes and variants of geomorphic evolution. In W. K. Jones, D. C. Culver, & J. Herman (Eds.), Re-published (modified) from 2004. *Epikarst*. Proceedings of the Symposium held October 1 through 4, 2003 Sheperdstown, West Virginia, USA. Karst Water Institute Special Publication 9, pp. 23–35. Retrieved from http://speleogenesis.info/pdf/SG5/SG5_artId3263.pdf
- McVoy, C. W., Said, W. P., Obeyseker, J., Van Arman, J. A., & Dreschel, T. W. (2011). *Landscapes and hydrology of the pre-drainage everglades*. Gainesville, FL: University Press of Florida, 342 pp. ISBN 13: 9780813035352.
- Meeder, J. F., & Harlem, P. W. (2010). Historic surface water discharge to Biscayne Bay via the Transverse Glades (TGs). (Oral) Greater Everglades Ecosystem Restoration (GEER) Conference, Naples, FL. <https://conference.ifas.ufl.edu/GEER2010/pdf/Abstract%20BOOK.pdf>
- Moore, W. S. (1982). Late Pleistocene history. In M. Ivanovich, & R. S. Harmon (Eds.), *Uranium series disequilibrium: Applications to environmental problems*. Oxford, UK: Oxford University Press, pp. 481–496. ISBN 0198544235.
- Mylroie, J. E., & Carew, J. L. (1988). Solution conduits as indicators of Late Quaternary sea-level position. *Quaternary Science Review*, 7, 55–64. ISBN 0813723000, 9780813723006.
- Mylroie, J. E., Jenson, J. W., Taborosi, D., Jocson, J. M. U., Vann, D. T., & Wexel, C. (2001). Karst features of Guam in terms of a general model of carbonate island karst. *Journal of Cave and Karst Studies*, 63, 9–22. Retrieved from <https://nss2013.caves.org/pub/journal/JCKS/PDF/V63/v63n1-Mylroie.pdf>
- Neal, A., Grasmueck, M., McNeil, D. F., Viggiano, D. A., & Eberli, G. P. (2008). Full-resolution 3D radar stratigraphy of complex oolitic sedimentary architecture: Miami Limestone, Florida, USA. *Journal of Sedimentary Research*, 78, 638–653.
- Parker, G. G. (1975). Hydrology of the pre-drainage system of the Everglades in southern Florida. In P. J. Gleason (Ed.), *Environments of South Florida present and past II*. Miami, FL: Miami Geological Society Memoir, 5, 18–27.
- Parker, G. G., & Cooke, C. W. (1944). Late Cenozoic geology of southern Florida, with a discussion of the ground water. *Florida Geological Survey Bulletin*, 27, 1–119.
- Parker, G. G., Ferguson, E., & Love, S. K. (1955). Water resources of Southern Florida. *United States Geological Survey Water Supply Paper*, 1255, 1–965.
- Perkins, R. D. (1977). Depositional framework of Pleistocene rocks of south Florida. Pt. 2. In *Quaternary sedimentation in South Florida*. *Geological Society America Memoir*, 147, 131–198.
- Plummer, L. N. (1975). Mixing of sea water with calcium carbonate groundwater. In E. H. T. Whitten (Ed.), *Quantitative studies in geological sciences*. *Geological Society America Memoir*, 142, 219–236. ISBN 0-8137-1142-8.
- Renken, R. A., Cunningham, K. J., Shapiro, A. M., Harvey, R. W., Zygnerski, M. R., Metge, D. W. ... Wacker, M. A. (2008). Pathogen and chemical transport in the karst limestone of the Biscayne aquifer: 1. Revised conceptualization of groundwater flow. *Water Resources Research*, 44(8), <https://doi.org/10.1029/2007WR006058>.
- Renken, R. A., Shapiro, A. M., Cunningham, K. J., Harvey, R. W., Metge, D. W., Zygnerski, M. A. ... Ryan, J. N. (2005). Assessing vulnerability of a municipal well field to contamination in a karst aquifer. *Environmental & Engineering Geosciences*, 4, 319–331. <https://doi.org/10.2113/11.4.319>.
- Robbin, D. M. (1984). A new Holocene sea level curve for the Upper Florida keys and Florida reef tract. In P. J. Gleason (Ed.), *Environments of South Florida: Present and past II* (pp. 437–458). Miami, FL: Miami Geological Society, Memoir 2.
- Ross, M., Sah, J., Meeder, J., Ruiz, P., & Telesnicki, G. (2013). Compositional effects of sea-level rise in a patchy landscape: the dynamics of tree islands in the southeastern coastal Everglades. *Wetlands*, 34, 91–100. <https://doi.org/10.1007/s13157-013-0376-2>.
- Sanford, S. (1909). Geology of southern Florida. Florida State Geological Survey, 2nd Annual Report, pp. 177–231.
- Shaler, N. S. (1890). The topography of Florida. *Harvard Collection, Museum Comparative Zoology Bulletin*, 16, 139–158.
- Shinn, E. A., Lidz, B. H., & Holmes, C. W. (1990). High-energy carbonate-sand accumulation, the quicksands, Southwest Florida keys. *Journal of Sedimentary Petrology*, 60, 952–967.
- Sklar, F. H., Meeder, J. F., Troxler, T. G., Dreschel, T., Davis, S. E., & Ruiz, P. L. (2019). Chapter 16 – The everglades: At the forefront of transition. In E. Wolanski, J. Day, M. Elliott, & R. Ramachandran (Eds.), *Coasts and estuaries – The future* (pp. 277–292). Elsevier. <https://doi.org/10.1016/B978-0-12-8144003-1.00016-2>.
- Sullivan, P. L., Price, R. M., Schedlbauer, J. L., Saha, A., & Gaiser, E. E. (2014). The influence of hydrologic restoration on groundwater-surface water interactions in a karst wetland, The Everglades (FL, USA). *Wetlands*, 34(Suppl. 1), 23–35. <https://doi.org/10.1007/s13157-013-0451-8>.
- Sweeting, M. M. (1973). *Karst landforms*. New York, NY: Columbia University Press, 362 pp.
- Vacher, H. L., & Mylroie, J. E. (2002). Eogenetic karst from the perspective of an equivalent porous medium. *Carbonates and Evaporates*, 17, 182–196. <https://doi.org/10.1007/BF03176484>.
- Wanless, H. R., Parkinson, R. W., & Tedesco, L. P. (1994). Sea level control on stability of everglades wetlands. In Davis, S., & Ogden, J. C. (Eds.), *Everglades: The ecosystem and its restoration* (pp. 199–223). Delray Beach, FL: St Lucie Press. ISBN 0-9634030-2-8.

- White, W. A. (1970). The geomorphology of the Florida Peninsula. *Florida Bureau of Geology Bulletin*, 51, 1–164. ufdc.ufl.edu/UF00000149/00001.
- Whitman, D., Zhang, K., Leatherman, S. P., & Robertson, W. (2003). An airborne laser topographic mapping application to hurricane storm surge hazard. *Earth science in the cities*, 56, 363–376.
- Zhang, K., Chen, S. C., Whitman, D., Shyu, M. L., Yan, J., & Zhang, C. (2003). A progressive morphological filter for removing non-ground measurements from airborne LIDAR data. *IEEE Transactions on Geoscience and Remote Sensing*, 41, 872–882. <http://users.cis.fiu.edu/~chens/PDF/TGRS.pdf>
- Zhang, K. and Whitman, D. (2005). Comparison of three algorithms for filtering airborne LIDAR data. *Photogrammetric Engineering and*

Remote Sensing, 71, 313–324. Retrieved from https://www.asprs.org/wp-content/uploads/pers/2005journal/mar/2005_mar_313-324.pdf

How to cite this article: Meeder JF, Harlem PW. Origin and development of true karst valleys in response to late Holocene sea-level change, the Transverse Glades of southeast Florida, USA. *Depositional Rec.* 2019;5:558–577. <https://doi.org/10.1002/dep2.84>